Effect of Surface Modification of Sisal Fibers on Water Absorption and Mechanical Properties of Polyaniline Composite

Tesfamariam Teklu ⓘ,[1,2] Lodrick M. Wangatia,[1] Esayas Alemayehu[3]

[1]School of Materials Science & Engineering, Jimma University Institute of Technology, Jimma, Ethiopia

[2]Department of Chemistry, College of Natural & Computational Sciences, Mekelle University, Mekelle, Ethiopia

[3]School of Civil & Environmental Engineering, Jimma University Institute of Technology, Jimma, Ethiopia

This article presents the surface modification of sisal (*Agave sisalana*) fibers by alkalization to tune up mechanical limitations of natural fibers-reinforced polymer composites associated with poor fiber-polymer matrix compatibility. Upon surface treatment, the fibers were surface coated with polyaniline through *in situ* oxidative polymerization to further enhance resistance to water absorption by introducing hydrophobic polymer backbone. Based on the results from spectroscopic and microscopic analyses, surface modification through alkalization is an effective approach to remove lignin and hemicellulose from the surface of sisal fibers. It also enhanced fiber-polymer matrix compatibility assured by a significant increase in tensile strength. Polyaniline deposition on the surface of sisal fibers was successful to introduce hydrophobic polymer backbone to the system to enhance resistance to water absorption, thereby increasing tensile strength significantly. POLYM. COMPOS., 00:000–000, 2017. © 2017 Society of Plastics Engineers

INTRODUCTION

Conducting polymers with polyaromatic backbone such as polypyrrole (PPy), polyaniline (PAni), and polythiophene (PTh) and their derivatives have captured the attention of scientific community owing to their extraordinary properties, including, but not limited to, the following: conductive coatings, rechargeable batteries, and ion-exchange characteristics. PAni is among the most widely used conducting polymers due to its oxygen and moisture stability and potential applications in many fields [1–3].

Even though PAni has very high chemical flexibility, the poor processability and low mechanical properties [4] limit some industrial applications. To further exploit the fascinating features of PAni, various approaches have been tested, including copolymerization, doping with functionalized protonic acids [5], blending with polymers [6–8], and coating on fibrous materials [9]. These processes offer better mechanical strength and improve processability of PAni [4, 10–12].

In the past few decades, an increasing interest arose to develop polymer-based composites reinforced with natural fibers which date back to the beginning of human civilizations when straw or grass was used to reinforce raw bricks from clay. Fibrous materials such as sisal, hemp, jute, and kenaf are progressively gaining ground in industrial applications for being plentiful, low environmental impact and presenting fairly good mechanical properties [13, 14]. Among various lignocellulosic fibers, sisal possesses interesting features, such as fairly coarse, moderate mechanical strength, resistance to deterioration in salt water, and low cost. These fascinating properties rendered sisal fiber as good reinforcing material in polymer matrices to make useful composites [15].

However, application of natural fibers as reinforcement for polymer composites has certain shortcomings: high moisture uptake and water absorption cause swelling which deteriorates mechanical strength and shortens the lifespan of composite materials [14, 16]. To make good use of sisal fiber as reinforcement in polymer composites, fiber-surface treatment must be carried out to obtain an enhanced interface between the sisal fiber and polymer matrices. Consequently, a surface modification through alkalization is desired to improve the affinity and adhesion between the surface of natural fiber and polymer-matrix phase [17], besides to removal of lignin, waxy substances, and other surface impurities.

Fiber-reinforced conducting polymer composites can be synthesized by *in situ* chemical oxidation [18–20], emulsion [21], electrochemical [22], and dispersion polymerization [23]. The *in situ* deposition of polymers on surface substrates has emerged as promising method to alleviate processability issues associated with polyaniline and prevent formation of aggregates [24] to maximize surface area. This can be achieved by mixing all components before polymerization or intercalation of monomer or oxidant into substrate followed by addition of second reactant.

Therefore, the work presented here is primarily centered to study the influence of surface modification by alkalization and polyaniline deposition on the surface of sisal fibers. Besides, effects of surface modification and polyaniline deposition on water absorption and mechanical properties of sisal fibers were investigated using Fourier-transform infrared spectroscopy (FTIR), ultraviolet–visible spectroscopy (UV–Vis), energy-dispersive X-ray spectroscopy (EDX), optical microscopy, scanning electron microscopy (SEM), and tensile testing machine.

EXPERIMENTAL METHODS

Reagents

The following reagents were of analytical grade and used without further purification: aniline (C_6H_7N), ferric chloride hexahydrate ($FeCl_3.6H_2O$), hydrochloric acid (HCl), sodium hydroxide (NaOH), and acetone (C_3H_6O) purchased from Merck Chemical Co. (Germany) through a local agency.

Materials

Sisal (*Agave sisalana*) was obtained from Mekelle, Northern Ethiopia. The fibers were extracted using manual process [25], and then they were air dried and washed with double distilled water, followed by acetone and finally dried in air at room temperature [26].

Surface Modifications

Sisal fibers were subjected to chemical cleaning process and soaked in 2 M NaOH solution for 2 h at room temperature [27, 28]. After surface modification through alkalization, fibers were washed thoroughly in pure water to remove excess alkali solution from the surface of the fibers and rinsed again with double distilled water [29]. Then, surface-modified sisal fibers were filtered on Whatman filter papers and oven dried at 60°C for 48 h [30].

Surface Coating of Sisal Fibers With Polyaniline

Five grams of sisal fibers was acidified in 0.2 M HCl solution to soak uniformly and facilitate diffusion of the monomer [31]. A 100 mL of 0.5 M aniline solution was added to the flask containing acidified fiber on continuous stirring to maintain uniformity throughout the system. Equal volume of 0.5 M $FeCl_3 \cdot 6H_2O$ oxidant solution was added to the mixture dropwise to initiate *in situ* oxidative polymerization and the reaction was allowed to continue for 12 h at room temperature [32]. Polyaniline-coated sisal fibers were filtered, and then washed with dilute HCl solution followed by double distilled water repeatedly until the filtrate became colorless to remove monomer and remaining oligomer impurities. Finally, it was oven dried at 60°C for 72 h [4].

Characterization and Testing

Fourier-Transform Infrared (FT-IR) Spectroscopy. Bruker Vector 22 Fourier-transform infrared spectrometer was used to record the spectra of untreated sisal fibers (USF), alkali-treated sisal fibers (TSF), and polyaniline-coated sisal fibers, PAni/USF, and PAni/TSF, samples to analyze the chemical structure of the fibers. Powder KBr disk technique was used in a spectral range of 4000–400 cm^{-1}.

Color Fastness Tests Coupled With UV–Visible Spectroscopy. PAni/USF and PAni/TSF were soaked in distilled water, nonphosphate detergent, and chloroform separately and subjected to color fastness test in Mesdan Auto Wash with a speed of 40 rpm at 60°C for 90 min washing time. The outwash was only used to extract the PAni from fibers; the amount of extracted PAni was then tested using PerkinElmer Lambda 9 UV–visible spectrophotometer in the wavelength region of 200–750 nm.

Scanning Electron Microscopy (SEM) and Energy-Dispersive X-Ray (EDX) Spectroscopy. Morphology of free sisal fibers (USF and TSF) and polyaniline-coated sisal fibers (PAni/USF and PAni/TSF) were observed using a highly customizable scanning electron microscope (JSM-IT300LV, JEOL, USA) coupled with a port for analytical attachment of energy-dispersive X-ray (EDX) spectrometry. The samples were gold coated by sputtering technique to avoid charging.

Fiber Fineness and Mechanical Property Testing. Fibers were photographed using Leica optical microscope fitted with a camera. The microscope had image analysis software which allowed measurement of the fiber diameter at various points. The diameter presented was an average of measurements taken at four different locations along the fiber length. Breaking load and extension at break of original length of 25 mm fiber samples were performed on Tinius Olsen H1KS single fiber strength testing machine.

Water Absorption Tests. Water absorption studies were performed using ASTM D 570–98 method with some modifications. Water absorption tests of untreated, alkali-modified, and polyaniline-coated sisal fibers were
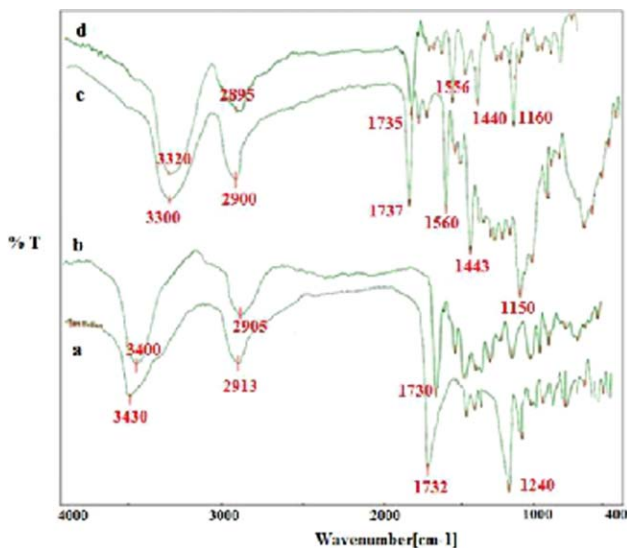
FIG. 1. FT-IR spectra of (a) USF, (b) TSF, (c) PAni/USF, and (d) PAni/TSF. [Color figure can be viewed at wileyonlinelibrary.com]

carried out by taking 1 g of each sample. Each sample was completely soaked in double distilled water at 25°C for about 12 h. At the end of the immersion periods, the specimens were removed from water, the surface water was wiped off using cotton cloth, and the wet-weight values were determined and reported in weight percent.

RESULTS AND DISCUSSION

Fourier-Transform Infrared (FT-IR) Spectroscopy

The FT-IR spectra of USF, TSF, and polyaniline-coated sisal fibers (PAni/USF and PAni/TSF) are presented in Fig. 1. A comparison of the spectra of USF, TSF, PAni/USF, and PAni/TSF reveals several peaks in common. The bands at 2913, 2905, 2900, and 2895 cm^{-1} for USF, TSF, PAni/USF, and PAni/USF, respectively, correspond to the C─H stretching vibrations of aliphatic hydrocarbons [33]. The peaks at 1732, 1730, 1737, and 1735 cm^{-1} correspond to the carbonyl stretching vibrations [34] of hemicellulose and lignin from sisal fibers. The absorption bands of TSF and PAni/TSF of C═O stretching at 1730 and 1735 cm^{-1} (Fig. 1b and d) are less intense compared to the bands of USF and PAni/USF, which clearly suggests that there is partial removal of hemicellulose from the surface of the fiber upon application of alkali treatment [14]. There is one notable difference between USF and TSF (Fig. 1a and b). A very strong peak at 1240 cm^{-1} in USF was totally disappeared from TSF sample. This strong absorption peak represents C─O stretching vibration of aryl groups from lignin which was removed on chemical treatment from TSF [35].

Polyaniline coating onto the surface of USF and TSF has revealed appearance of unique peaks. Strong bands lying between 1150 and 1160 cm^{-1} in PAni/USF and PAni/TSF are characteristic features of PAni conductivity as a result of electron delocalization [36]. Deposition of polyaniline on the surface of sisal fibers signifies presence of benzoid ring (N═B═N) around 1440–1443 cm^{-1} [37] and quinoid ring (N═Q═N) vibration from 1556 to 1560 cm^{-1}, indicating that PAni is in its oxidized form, emeraldine salt [38, 39]. There are no benzoid and quinoid bands on USF and TSF. This further confirmed that polyaniline was successfully coated on the surface of sisal fibers.

Moreover, characteristic peaks of N─H stretching vibration of amine groups from PAni/USF and PAni/TSF appear around 3300 and 3320 cm^{-1}, respectively, signifying deposition of polyaniline on the surface of the fibers [40]. Comparing the FT-IR spectra of free sisal fibers with polyaniline-coated ones, there is remarkable difference in the higher absorption bands. Free fibers (Fig. 1a and b) have bands in common above 3400 cm^{-1} which belongs to the O─H stretching vibrations of intermolecular and intramolecular H bonds from cellulose. The effect of surface modification of sisal fibers through alkalization is clearly visualized by exposing cellulose compared to untreated fibers as the O─H absorption band of TSF is more intense to that of USF [14].

Color Fastness Coupled With UV–Visible Spectroscopy

Color fastness, a term usually used in the context of textiles, was applied to sisal fibers coated with polyaniline by washing in water and nonphosphate detergent solution. All the samples did not show any sign of loss of color as evidenced by no color change of the filtrate which was visually identified. Contrary to this, color change was easily observed from greenish to blue on the surface of the sisal fibers when washed in the later solution which is a confirmation that emeraldine salt has changed to emeraldine base. It is obvious that the detergent employed is alkaline media, approximately pH ≥ 10, causing deprotonation of polyaniline and, consequently, a color change occurred [18, 41, 42]. Washing polyaniline-coated sisal fibers in chloroform solution gave greenish filtrate solution alongside fading polyaniline color on the surface of the fibers.

The filtrate obtained after washing was subjected to UV–vis spectroscopy to establish the concentration of PAni which is a reflection of color fastness. As the samples where water and detergent were used to wash had insignificant color change, their results were neglected and only filtrates from the samples washed with chloroform were tested. In the UV–visible absorption spectra of PAni/USF and PAni/TSF filtrate from chloroform solution, there are three distinct bands. The peak characteristic around 300 nm (Fig. 2d) belongs to π–π* transition of benzoid ring of PAni backbone and a peak at 475 nm assigned to the polaron–π* band. There is one peak at 680 nm peculiar to PAni/TSF belonging to π–polaronic transitions which is absent in all the other forms. The last two bands are clear evidences confirming PAni exists in its green, conducting emeraldine salt [43, 44]. It is worthy to compare the absorption spectra of PAni/USF and PAni/TSF (Fig. 2c and d), which clearly
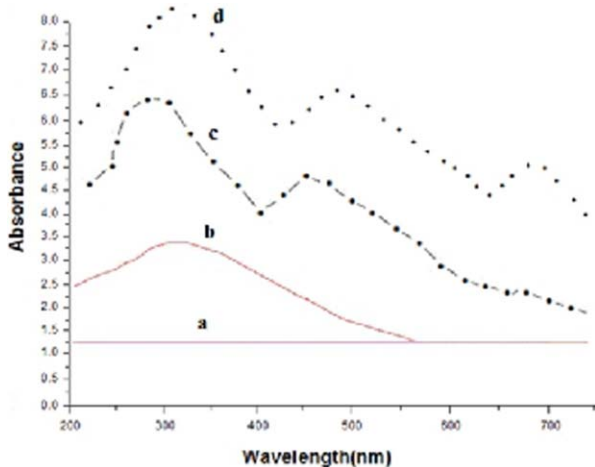
FIG. 2. UV–Vis spectra of (a) PAni/USF in water, (b) PAni/USF in nonphosphate detergent, (c) PAni/USF in chloroform, and (d) PAni/TSF in chloroform. [Color figure can be viewed at wileyonlinelibrary.com]

shows remarkable differences. The shift of π–π^* and polaron–π^* to the lower band and the absence of a peak around 680 nm in PAni/USF (Fig. 2c) is an indication of poor surface interaction between the fiber and PAni. This phenomenon is resulted in high-energy transitions which causes disappearance of π–polaron band [45]. The filtrate from PAni/USF washing in nonphosphate detergent gives diffuse and broadened peak around 300 nm (Fig. 2b). There is no any sort of absorption peak for PAni/USF in distilled water (Fig. 2a). It is a confirmation that PAni is insoluble in water.

Surface Morphology

Comparison of the micrographs of untreated (USF) and chemically modified sisal fibers (TSF) (Fig. 3a and b) shows a considerable difference. The surface morphology of USF revealed a major section of the surface is irregular with a variety of debris, cracks, voids, and entanglements. Unlike USF, SEM micrograph of TSF indicates the surface is clean with a reduced debris, microcracks, and overgrowths. This is absolutely due to the removal of lignin and part of hemicellulose as a result of surface modification through alkalization from the surface and the interspaces [46]. The corresponding EDX spectra of USF (Fig. 4a) further confirmed existence of impurities such as aluminum and sulfur incorporated with the fiber. These impurities may be introduced from reactants, solvents, and the fiber itself.

The SEM micrographs of PAni/USF and PAni/TSF (Fig. 3c and d) shows that surface of PAni/USF and PAni/TSF is relatively clean which has changed a lot compared to that of USF. This morphological variation might be as a result of surface deposition of polyaniline on sisal fibers. Of course, SEM microstructure of PAni/TSF is very clean compared to the other microstructures. This may suggest surface modification through alkalization is efficient to remove surface impurities, voids, and cracks. The EDX spectra (Fig. 4c and d) further proved impurities such as aluminum and sulfur were successfully removed during the process of *in situ* oxidative polymerization. These spectra confirmed polyaniline was successfully deposited on the surface of sisal fibers, which show detection of intense chlorine and nitrogen from polyaniline backbone [45].
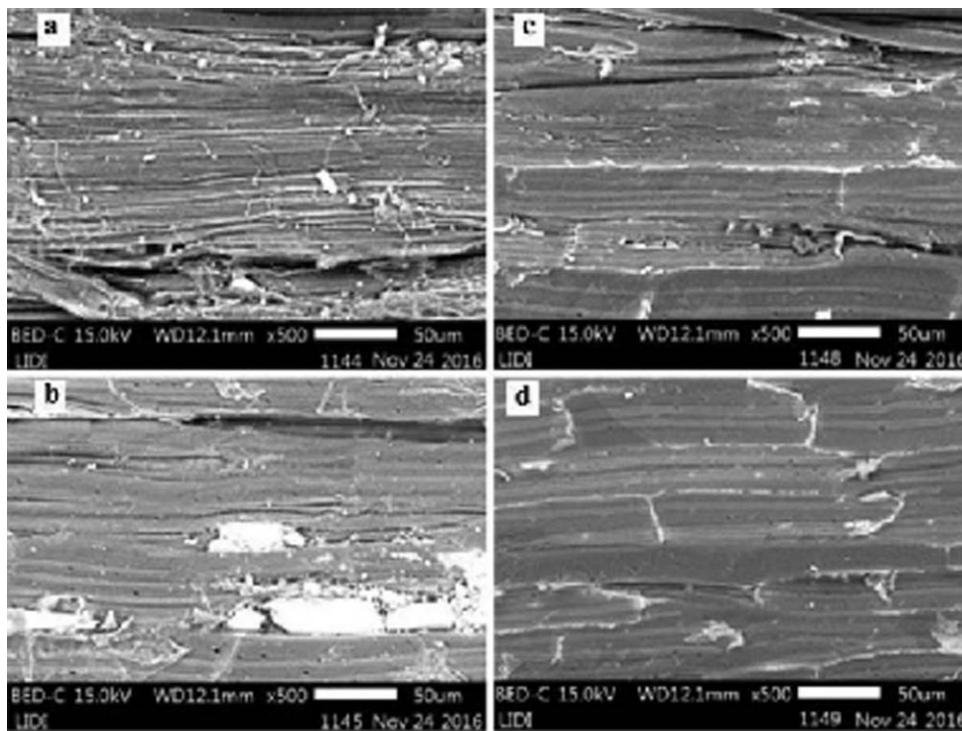

FIG. 3. SEM micrographs of (a) USF, (b) TSF, (c) PAni/USF, and (d) PAni/TSF.
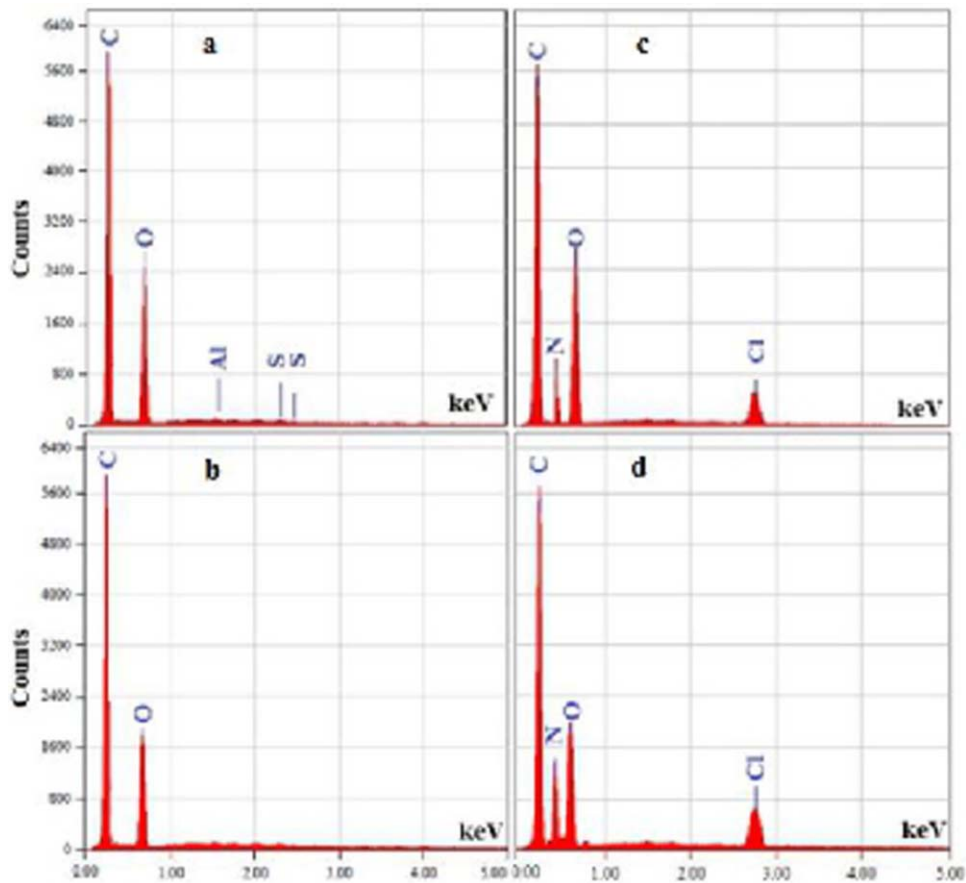
FIG. 4. EDX spectra of (a) USF, (b) TSF, (c) PAni/USF, and (d) PAni/TSF. [Color figure can be viewed at wileyonlinelibrary.com]

Fiber Fineness and Mechanical Properties

The mean value of diameters measured using computerized image analysis software for sisal fibers of USF, TSF, PAni/USF, and PAni/TSF was 291, 249, 282, and 262 μm, respectively. These values are in good agreement with results found in other research works which ranges from 100 to 300 μm [13, 47–49]. Each diameter of a given fiber (Fig. 5) revealed that there is slight variation among the measured values throughout the given length. Even though it is difficult to conclude that surface modification through alkalization is a prominent factor that significantly affects the diameter [50], the mean value of measured diameters was greatly reduced to 249 μm compared to that of USF which is 291 μm. This might be associated with the removal of lignin, hemicellulose, and waxy substances.

One of the main difficulties in engineering applications of lignocellulosic fibers is lack of precise measurement of diameter as they are nonuniform throughout the length. This in turn causes heterogeneity on cross-sectional area and common mechanical properties [51, 52]. Most natural fibers generally possess variable and irregular cross-sections which can lead to errors in computation of mechanical properties. Theoretically, sisal fibers are assumed as solids and their cross-section is nearly cylindrical in shape. Cross-sectional area (A) of sisal fibers was calculated using Eq. 1 [53]:

$$A = \pi \frac{d^2}{4} \tag{1}$$

where A is the cross-sectional area and d is the diameter of sisal fibers under study.

Elongation at break is a parameter used to analyze how much natural fibers are resistant to an applied load. TSF was found to have the highest elongation of 3.9% (Table 1).
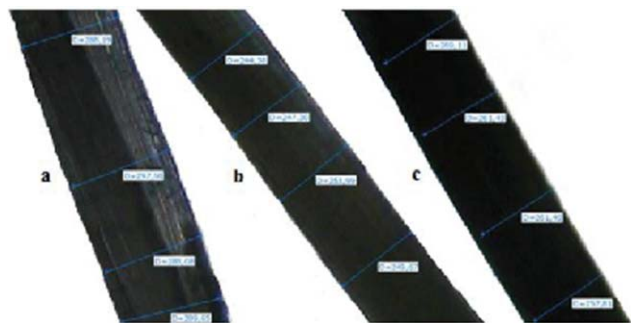

FIG. 5. Optical microscopy image of (a) USF, (b) TSF, and (c) PAni/TSF. [Color figure can be viewed at wileyonlinelibrary.com]

TABLE 1. Physical and mechanical properties of USF, TSF, PAni/USF, and PAni/TSF.

Sample	Diameter, μm	Cross-sectional area, mm²	Elongation at break, %	Water absorption (12 h), %
USF	291	0.067	2.5	20.9
TSF	249	0.049	3.9	9.8
PAni/USF	282	0.063	2.8	3.5
PAni/TSF	262	0.054	3.1	2.52

The surface modification by alkali treatment on the fiber is responsible for enhanced elongation at break [54].

The tensile strength results of free and polyaniline-coated sisal fibers are summarized in Fig. 6. It is interesting to note that TSF showed higher tensile strength than USF and polyaniline-coated sisal fibers, PAni/USF, and PAni/TSF, this could have resulted from the fact that tensile strength is a factor of fiber diameter where thinner fibers have higher strength. The same argument is true when PAni/USF tensile strength is compared to PAni/TSF [48, 55, 56].

Water Absorption

The water absorption values of USF, TSF, and PAni-coated sisal fibers calculated by the weight difference are presented in Table 1. The results show that USF absorbs more water suggesting that the surface chemistry is extremely hydrophilic due to the presence of hydroxyl rich cellulose giving high affinity to take up high amount of moisture [57, 58]. The water absorption was drastically reduced from 20.9% to 9.8% after surface treating the fibers. This is a clear indication that alkalization process reduces the water absorption which could probably be attributed to removal of lignin from the fibers [46]. Coating the fibers with polyaniline was a better method of reducing the fiber water absorption as compared to surface treatment, as PAni/USF samples had much lower absorption of 3.5% compared to TSF 9.8%. Lowest absorption was obtained on combining surface treatment with polyaniline coating, the PAni/TSF absorption was 2.52% [59].
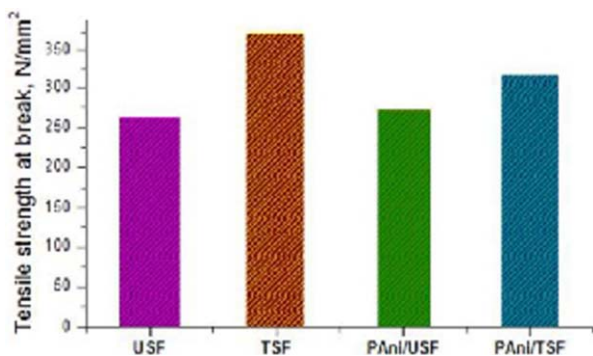

FIG. 6. Tensile strength at break of free and polyaniline-coated sisal fibers. [Color figure can be viewed at wileyonlinelibrary.com]

CONCLUSIONS

Based on the results from different characterization techniques such as FT-IR, UV–vis, and EDX confirmed that *in situ* oxidative polymerization is successfully proved to introduce polyaniline on the surface of sisal fibers which further proved to enhance resistance to water absorption, thereby enhancing mechanical strength.

Surface modification upon alkalization assured certain percentages of impurities, variety of microcracks, and overgrowths were successfully removed from the surface of sisal fibers. This process showed a significant increase in resistance to water absorption. It was also successful enough to enhance fiber–polymer matrix compatibility upon subsequent polyaniline coating. Both polyaniline coating and surface modification enhanced resistance to water absorption along with mechanical behavior of composites compared to bare sisal fibers.

Therefore, sisal fibers reinforced polyaniline composite can be future foundations for different applications such as water treatment systems, electromagnetic shielding, and electronics.

REFERENCES

1. S.L. Goyal, S. Sharma, D. Jain, D. Kumar, and N. Kishore, *Adv. Appl. Sci. Res.*, **6**, 89 (2015).

2. E. Hossein and A.M. Seiedeh, *J. Vinyl. Addit. Technol.*, 170 (2010), doi: 10.1002/vnl.20238.

3. N.K. Madi, J. Bhadra, N.J. Al-Thani, A. Alashraf, D. Abdulmalik, and I. Al-Qaradawi, *J. Vinyl. Addit. Technol.*, doi: 10.1002/vnl.21549, 1 (2016).

4. V. Bajgar, M. Penhaker, L. Martinková, A. Pavlovic, P. Bober, M. Trchová, and J. Stejskal, *Sensors*, **16**, 1 (2016).

5. S. Kim, J.M. Ko, and I.J. Chung, *Polym. Adv. Technol.*, **7**, 599 (1996).

6. F.G. Souza, Jr, B.G. Soares, G.L. Mantovani, A. Manjunath, H. Somashekarappa, and R. Somashekar, Siddaramaiah, *Polymer*, **47**, 2163 (2006).

7. S. Kutanis, M. Karakisla, U. Akbulut, and M. Sacak, *Compos. A*, **38**, 609 (2007).

8. J.D. Sudha and S. Sivakala, *Colloids Polym. Sci.*, 1 (2009). doi: 10.1007/s00396-009-2101-5.

9. S. Sakthivel and A. Boopathi, *J. Chem. Chem. Sci.*, **5**, 111 (2015).

10. E. Hossein and H.K. Reza, *J. Eng. Sci. Technol.*, **3**, 146 (2008).

11. R. Hirase, T. Shikata, and M. Shirai, *Synth. Met.*, **146**, 73 (2004).

12. A.J. Patil and S.C. Deogaonkar, *Text. Res. J.*, **82**, 1517 (2012).

13. D.S. da Costa, J.A. Souza, D.S. Costa, and P.S. de Oliveira, *Int. J. Eng. Innovative Technol.*, **4**, 70 (2015).

14. N. Sgriccia, M.C. Hawley, and M. Misra, *Compos. A*, **39**, 1632 (2008).

15. M. Benítez-Guerrero, L.A. Pérez-Maqueda, R. Artiaga, P.E. Sánchez-Jiménez, and J. Pascual-Cosp, *J. Nat. Fibers*, 1 (2016). doi: 10.1080/15440478.2015.1137529.

16. G. Toriz, F. Denes, and R.A. Young, *Polym. Compos.*, **23**, 806 (2002).

17. M. Tlijania, A. Gouadriab, R. Benyounesc, J. f. Durastantid, and A. Mazioude, *Global J. Sci. Front. Res.*, **14**, 29 (2014).

18. J. Molina, M.F. Esteves, J. Fernández, J. Bonastre, and F. Cases, *Eur. Polym. J.*, **47**, 2003 (2011).

19. X. Jiang, T. Dai, and Y. Lu, *Iran Polym. J.*, **17**, 645 (2008).

20. A. Kaynak, S.S. Najar, and R.C. Foitzik, *Synth. Met.*, **158**, 1 (2008).

21. A. Reung-U-Rai, A. Prom-Jun, W. Prissanaroon-Ouajai, and S. Ouajai, *J. Met. Mater. Miner.*, **18**, 27 (2008).

22. X. Yang, T. Dai, Z. Zhu, and Y. Lu, *Polymer*, **48**, 4021 (2007).

23. A.Y. Men'shikova, B.M. Shabsel's, and T.G. Evseeva, *Russ. J. Appl. Chem.*, **76**, 851 (2003).

24. F. Kanwal, R. Rehman, J. Anwar, and M. Saeed, *Asian J. Chem.*, **25**, 2399 (2013).

25. P. Kolte, A. Daberao, and A.M. Sharma, *Text. Rev.*, **7**, 1 (2012).

26. A. Hulle, P. Kadole, and P. Katkar, *Fibers*, **3**, 64 (2015).

27. A.K. Mohanty, M. Misra, and L.T. Drzal, *Compos. Interfaces*, **8**, 313 (2001).

28. S. Mishra, M. Misra, S.S. Tripathy, and S.K. Naya, *Polym. Compos.*, **23**, 164 (2002).

29. J.T. Kim, and A.N. Netravali, *Compos. A*, **41**, 1245 (2010).

30. J.P. Siregar, S.M. Sapuan, M.-A. Rahman, and H.-K. Zaman, *J. Food Agric. Environ.*, **8**, 1103 (2010).

31. F.Z. Engin and I. Usta, *Text. Res. J.*, **84**, 903 (2014).

32. S.I. Razak, A.L. Ahmad, S.H. Zein, and A.R. Boccaccini, *Scr. Mater.*, **61**, 592 (2009).

33. M.A. Sawpan, K.L. Pickering, and A. Fernyhough, *Compos. A*, **42**, 888 (2011).

34. P. Ganan, S. Garbizu, R. Llano-Ponte, and I. Mondragon, *Polym. Compos.*, **26**, 349 (2005).

35. M. Troedec, D. Sedan, C. Peyratout, J. Bonnet, A. Smith, R. Guinebretiere, V. Gloaguen, and P. Krausz, *Compos. A*, **39**, 514 (2008).

36. H. Xia and Q. Wang, *J. Appl. Polym. Sci.*, **87**, 1811 (2003).

37. S. Quillard, G. Louarn, S. Lefrant, and A.G. MacDiarmid, *Phys. Rev. B Condens. Matter.*, **50**, 12496 (1994).

38. P. Chowdhury and B. Saha, *Indian J. Chem. Technol.*, **12**, 671 (2005).

39. F. Kanwal, R. Rehman, J. Anwar, and M. Saeed, *J. Chem. Soc. Pak.*, **34**, 1134 (2012).

40. J. Vivekanandan, V. Ponnusamy, and A. Mahudeswaran, *Arch. Appl. Sci. Res.*, **3**, 147 (2011).

41. K.W. Oh, K.H. Hong, and S.H. Kim, *J. Appl. Polym. Sci.*, **74**, 2094 (1999).

42. N. Onar, A.C. Aksit, M.F. Ebeoglugil, I. Birlik, E. Celik, and I. Ozdemir, *J. Appl. Polym. Sci.*, **114**, 2003 (2009).

43. S. Ito, K. Murata, S. Teshima, R. Aizawa, Y. Asako, K. Takahashi, and B.M. Hoffman, *Synth. Met.*, **96**, 161 (1998).

44. J. Fernando and C. Vedhi, *Int. J. Sci. Technol.*, **3**, 166 (2015).

45. S.I. Razak, W.A. Rahman, S. Hashim, and M.Y. Yahya, *Compos. Interfaces*, **19**, 365 (2012).

46. S. Mishra, M. Misra, S.S. Tripathy, S.K. Naya, and A.K. Mohanty, *Macromol. Mater. Eng.*, **286**, 107 (2001).

47. Y. Li, Y.-W. Mai, and L. Ye, *Compos. Sci. Technol.*, **60**, 2037 (2000).

48. M.A. Martins and I. Joekes, *J. Appl. Polym. Sci.*, **89**, 2507 (2003).

49. E.T. Bisanda and M.P. Ansell, *Compos. Sci. Technol.*, **41**, 165 (1991).

50. S.C. Amico, T.H. Sydenstricker, and P.C. da Silva, *Met. Mater. Process.*, **17**, 233 (2005).

51. A.K. Bledzki and J. Gassan, *Prog. Polym. Sci.*, **4**, 221 (1999).

52. A.K. Mohanty, M. Misra, and L.T. Drzal, *J. Polym. Environ.*, **10**, 9 (2002).

53. S.N. Monteiro, K.G. Satyanarayana, A.S. Ferreira, D.C. Nascimento, F.P. Lopes, I.L. Silva, A.B. Bevitori, W.P. Inácio, J.B. Neto, and T.G. Portela, *Rev. Mater.*, **15**, 488 (2011).

54. M.Z. Rong, M.Q. Zhang, Y. Liu, G.C. Yang, and H.M. Zeng, *Compos. Sci. Technol.*, **61**, 1437 (2001).

55. K. Joseph, S. Thomas, and C. Pavithran, *Polymer*, **37**, 5139 (1996).

56. W.P. Inacio, F.P. Lopes, and S.N. Monteiro, *Rev. Mater.*, **15**, 124 (2010).

57. T. Fakhrul and M.A. Islam, *Procedia Eng.*, **56**, 795 (2013).

58. C. Girisha, Sanjeevamurthy, and G.R. Srinivas, *Int. J. Eng. Innovative Technol.*, **2**, 1 (2012).

59. W. He, J. Li, J. Tian, H. Jing, and Y. Li, *Polym. Compos.*, 1 (2016). doi: 10.1002/pc.23966.